Current Biology 19, 140–145, January 27, 2009 ©2009 Elsevier Ltd All rights reserved DOI 10.1016/j.cub.2008.12.030

Report

Septin-Mediated Uniform Bracing of Phospholipid Membranes

Yohko Tanaka-Takiguchi,[1] Makato Kinoshita,[2] and Kingo Takiguchi[1,*]
[1]Department of Molecular Biology
School of Science
Nagoya University
Nagoya, 464-8602
Japan
[2]Biochemistry and Cell Biology Unit
Kyoto University Graduate School of Medicine
Kyoto 606-8501
Japan

Summary

Cell shape is determined by the interplay between the lipid bilayer and the underlying network of protein polymers [1]. We explored unknown determinants involved in cell morphogenesis as factors that transform phospholipid-based liposomes (diameter 5–20 μm). Unlabeled giant liposomes, observed through dark-field optics, were metastable in an aqueous suspension. In contrast, liposomes robustly protruded uniform tubules immediately after the addition of a brain extract to the suspension. The tubulation reaction was greatly facilitated when the liposomes contained PIP or PIP2. Biochemical analysis of the brain extract revealed that heteromeric complexes of septins, a family of polymerizing GTP/GDP-binding proteins, are responsible for the membrane transformation. Ultrastructural analysis established that each membrane tubule (diameter 0.43 ± 0.079 μm) is braced by a circumferential array of septin filaments. Although submembranous septin assemblies are associated with diverse cortical morphogenesis from yeast to mammals [2–5], the biophysical basis for the septin-membrane interplay remains largely unknown. Further, there is a biochemical discrepancy between the fast septin remodeling in cells and their slow self-assembly in vitro [6, 7]. This membrane-facilitated fast septin assembly demonstrated for the first time by our unique experimental system should provide important clues to characterize these processes.

Results and Discussion

Real-Time Observation of Giant Liposomal Transformation

Cells control the shape of phospholipid membranes by lipophilic proteins [8] and by cytoskeletal polymers [1, 9]. The BAR and F-BAR/EFC domain proteins are involved in endocytosis [10–13] and Alix/AIP-1 is involved in endosomal sorting and membrane budding [14]. Apart from those local membrane-transformation events, the molecular basis of global membrane transformation remains unknown, except for membrane displacement by tubulin and actin polymers [1, 9, 15]. To address the biophysical basis of global membrane transformation, we developed a dark-field video microscopy system and observed unlabelled large liposomes of various phospholipid compositions [15–18].

This unique system revealed that giant liposomes composed of a neutral phospholipid (phosphatidylcholine, PC) and inositol phospholipid (phosphatidylinositol [PI], phosphatidylinositol-4-monophosphate [PIP], or -4, 5-bisphosphates [PIP2]) are metastable in a physiological buffer (Figure 1A, "Control"), but they transform in response to an extract from porcine brain (Figure 1A, "+ Extract"). The brain extract consistently and rapidly induced the protrusion of multiple tubules from the majority of giant liposomes composed of PC and PI at a molar ratio of 1:1 (PC-PI liposomes). Each tubule was a continuous extension from the spherical part of a liposome, judging from the observations that the diameter of the liposome became smaller as the tubules elongated (Figure 1B, and see Supplemental Movies available online) and that the entire structure was homogeneously labeled with a lipophilic dye (Figure 1C). Liposomes containing acidic phospholipids in place of PI, such as phosphatidic acid (PA), phosphatidylglycerol (PG), or phosphatidylserine (PS), did not transform (data not shown), which indicates a specific requirement of PI for the phenomenon. Of note, the transformation was significantly more robust when PIP or PIP2 was supplemented in the liposomes (Figure 1D), which suggested an underlying biochemical interaction between phosphorylated PIs and unknown factors derived from the brain extract.

Quantitative analysis indicated that the number of protrusion sites per liposome increased until the liposomal surface was fully occupied by the existing tubules (Figure 1E and data not shown). The rate of tubule elongation was biphasic in the presence of excess brain extract, with a rapid initial phase up to a certain length (3.1 ± 1.2 μm, average ± standard deviation [SD], n = 20), followed by a slow but stable growth phase that lasted until the depletion of the available surface. The overall kinetics of the process is consistent with our previous observation that stable tubular growth is ensured after reaching a critical length of ~3 μm [19]. Together, these data demonstrate that the brain extract-induced tubulation is a saturable and self-limiting process resulting from the limited reactive surface areas of giant liposomes.

Identification of the Factor Responsible for the Membrane Transformation

To identify the factor(s) responsible for the membrane-transforming activity, we fractionated the brain extract by cation exchange and hydroxyapatite (HA) column chromatography. The biophysical activity was consistently concentrated in a specific fraction from the HA column (No. 11, total protein concentration, 0.1 mg/ml) and in neighboring fractions (Figure S1). Gel electrophoresis and Coomassie brilliant blue (CBB) staining visualized multiple proteinaceous components in each fraction. The biophysical activity (estimated from the number and length of the tubules) correlated with the amount of a 210 kDa band and a cluster of 40–50 kDa bands (Figure S1). By mass spectrometry and immunoblot analyses, we identified these bands as fodrin/spectrin and septins (Sept2, 3, 5, 7, and 11), respectively (Figure S2). Additionally, an active fraction similarly purified from rat brain also contained both fodrin

*Correspondence: j46037a@nucc.cc.nagoya-u.ac.jp

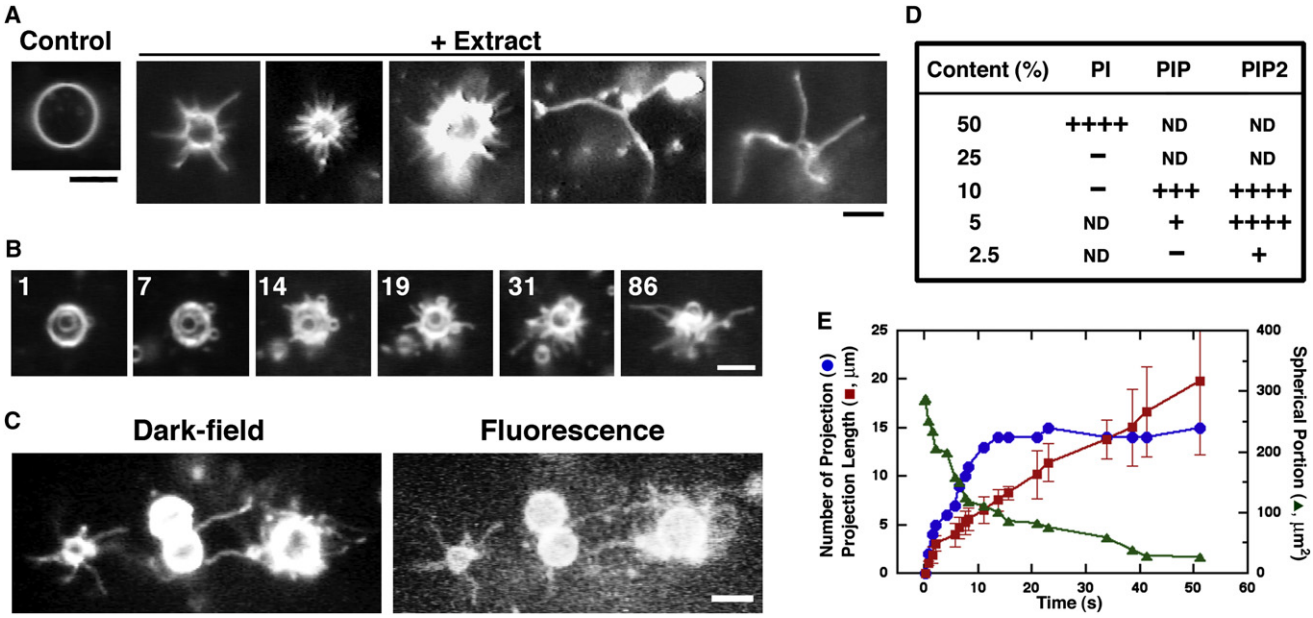

Figure 1. Tubulation of Giant Liposomes Induced by a Brain Extract

(A) Dark-field micrographs of PC-PI liposomes in the absence ("Control") or presence of a porcine brain extract. The extract induced prompt and robust tubulation from the liposomes, which were otherwise metastable.

(B) Time-lapse images of multiple tubulation from a shrinking giant liposome. The time after the start of observation is denoted in seconds. See also Movies S1 and S2.

(C) Fluorescence labeling of the tubulated liposome membrane with a lipophilic dye, DiI-C18. The fluorescence image (right) obtained immediately after the recording of the dark-field image (left) indicates that the tubules are continuous protrusions from the liposomes. Note an advantage of the dark-field optics by the higher contrast. Scale bars in (A)–(C) represent 10 μm.

(D) Requirement of PI, PIP, and PIP2 for the tubulation of giant liposomes. The degree of tubulation by the active fraction of the porcine brain extract (Figure S1B, No. 11) was semiquantified from the dark-field micrographs of giant liposomes composed of PC and varying concentrations (mol %) of PI, PIP, or PIP2: ++++, ~100% liposomes with >5 tubules or completely transformed into tubules; +++, >90% liposomes with >5 tubules; ++, >50% liposomes with a few tubules; +, >10% liposomes with ≥1 tubules; −, no tubulation observed; ND, not determined.

(E) Time course of a typical tubulation process. The number (blue circles) and length (μm, red squares, error bars for SD) of growing tubules and the shrinking spherical area (μm^2, green triangles) were estimated from a dark-field image sequence of a typical tubulating liposome (e.g., [B]) and plotted over time. The time when the first tubular projection was observed is defined as time 0.

and septins (Figure S3). Coimmunodepletion of the septins in heteromeric complexes from HA fraction No. 11 (HA No. 11) with an anti-Sept7 antibody abolished the tubulation, but attempts to similarly deplete fodrin/spectrin with commercially available antibodies failed for unknown reasons (Figure 2A and Figure S4, and data not shown).

Although a possible tubulation activity of fodrin/spectrin can not be excluded, the following pieces of evidence consistently indicate that septin complexes are the major tubulation factors in the active fraction. Septins are GTP-binding proteins purified from diverse eukaryotic cells as filamentous heteromeric complexes [6, 20]. Septin filaments assemble into diverse higher-order structures in vivo and in vitro, such as linear/circular/spiral bundles or gauze-like planar arrays underlying yeast plasma membranes [21]. The unique biochemical properties of septins have been implicated in a variety of membrane transformation/organization events in vivo, such as bud neck morphogenesis and asymmetric compartmentalization between dividing yeast cells, dendritic spine morphogenesis of neurons, cortical organization in mammalian spermatozoa and lymphocytes, and phagocytosis [3, 21–27]. These facts also exemplify the biological significance and uniqueness of the septin-membrane interplay, direct or indirect.

BAR domain proteins, some of which have been established as tubulating factors for smaller liposomes (diameter ≤ 0.1 μm), are unlikely to contribute to the transformation of the giant PC-PI liposomes for the following reasons. (1) In the active fraction of the brain extract (HA No. 11), amphiphysin was barely detectable, and dynamin and endophilin were undetectable by immunoblot (Figures S2, S4, and S5). (2) Immunodepletion of the three BAR domain proteins did not abolish the tubulation activity of the active fraction (Figure 2A; Figures S4 and S5). (3) BAR domain proteins do not specifically require inositol phospholipids for tubulation [28], whereas the active fraction does. Collectively, we concluded that septin complexes, but not BAR domain proteins, are essential components of the brain fraction for the inositol phospholipid-dependent transformation of giant liposomes with gentle curvature.

Next, we tested whether a pure septin complex alone is sufficient for the biophysical activity by using recombinant heterooligomers of human septin subunits Sept2, Sept6, and Sept7 (Figure S6) [6, 21]. Immediately after the addition of the recombinant Sept2/6/7 complex to a giant liposome suspension, a similar tubulation was recapitulated, which was more consistent when supplemented with excess GTP or GDP (Figure 2B). These data do not necessarily indicate that nucleotide exchange and/or hydrolysis are required for the tubulation, because (1) some of the purified septin subunits are known to be in apo-forms because of the spontaneous release of bound nucleotide during the purification process [6, 7, 29], and (2) either GTP- or GDP-bound Sept2 can form head-to-head (NC) dimers, although apo-Sept2 cannot [29].

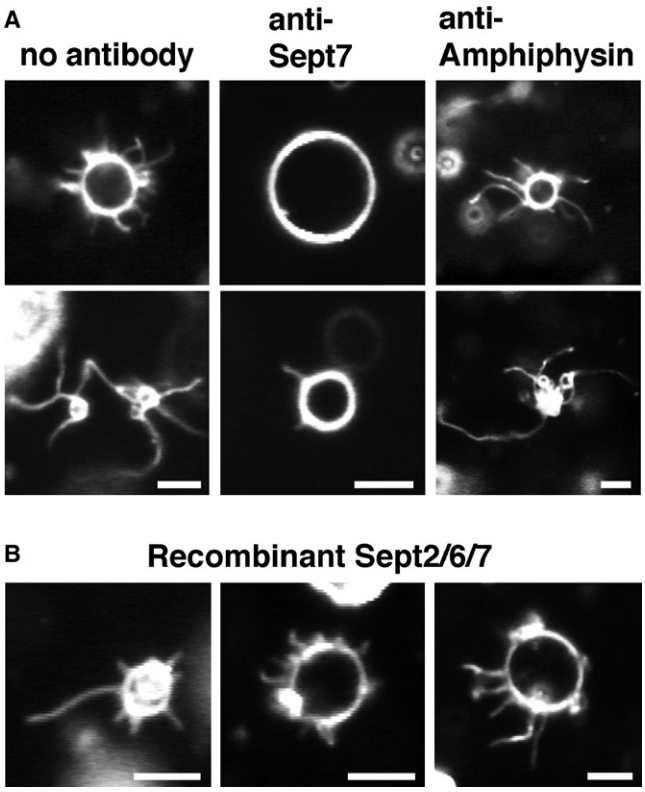

Figure 2. Septin Complexes Identified in the Active Fraction Are Necessary and Sufficient for the Tubulation of Giant PC-PI Liposomes

(A) The active fraction (HA No. 11, Figure S1) was immunodepleted with anti-Sept7 or with anti-amphiphysin antibody (Figure S4), and the residual tubulation activity was assayed as in Figure 1. Two representative images of different liposomes are shown for each case. Left: The mock-depleted active fraction (without antibody, with Protein A-conjugated resin alone) retained the full tubulation activity. Center: Immunodepletion of Sept7-containing septin complexes from the active fraction essentially abolished tubulation activity. Right: Immunodepletion of amphiphysin did not affect the tubulation activity.

(B) Representative images of giant PC-PI liposomes tubulated by recombinant Sept2/6/7 complexes (final concentration 0.36 mM, hexamer-base) plus 1 mM GTP. Neither GTP nor GDP alone had transforming activity. The recombinant Sept2/6/7 with or without GTP or GDP adhered to liposomes and formed arrays but did not protrude tubules as robustly as did the brain extract. Thus, the tubulation may require additional conditions such as the modification of septin polypeptides, composition or heterogeneity of septin complexes, substoichiometric nonseptin proteins, nonproteinaceous molecules, etc.

Scale bars represent 10 μm.

Thus, the additional nucleotide may replenish apo-Sept2 for the formation and/or stabilization of the NC dimer interface in the Sept7/6/2-2/6/7 hexamer [29].

A previous report showed that replacing two basic amino acid residues near the P loop with alanines abolished the interaction of GST-tagged Sept4/H5 (a Sept2 paralog) with phospholipids [30], and similar results were shown in a few yeast septin subunits [31]. Intriguingly however, a mutant complex $Sept2^{K33A,K34A}$/Sept6/$Sept7^{K27A,R28A}$, which contains the corresponding mutations, retained the liposome-binding and polymerizing activities (Figure S7). Hence each subunit of the mutant complex has only one or two basic residues in the region, and other regions may be responsible for the interaction with phospholipids in complexes. Alternatively, it is also possible that mutations that abolish the binding of single subunits to liposomes may retain enough affinity to bind when the mutant proteins are in large filaments.

Ultrastructural Analysis of the Transformed Liposomes

The tubules induced by the brain extract or by the pure septin complex appeared more rigid than the physicochemically induced tubules [15, 17, 19], demonstrating that the septin filaments assemble on the liposomal template and transform the spherical membrane into rigid tubules. Electron microscopy (EM) unequivocally revealed that the tubular parts of the transformed liposomes are trussed with circumferential arrays of septin filaments, which were frequently paired (diameter of a pair: 11 nm) or in wider bundles (Figures 3A–3E). Considering the slow self-assembly kinetics of septin oligomers in vitro (in hours) even in the presence of excess GTP or GDP [6, 7], these data also indicate that membranous platforms significantly facilitate the more rapid septin filament elongation, pairing, and array formation (in tens of seconds). Furthermore, the diameter of the tubules (0.43 ± 0.079 μm; Figure 3G) was close to the inner diameter of circular septin bundles self-assembled in vitro [6, 7]. We speculate that adherence onto a lipid template concentrates the septin rods and filaments in a spatially constrained, orientationally ordered manner, which cooperatively accelerates the filament elongation and lateral interaction (Figure 3H). The intrinsically favored curvature of the septin filament array, as is compatible with the structural flexibility at the NC dimer interface between the Sept2 subunits in each Sept7/6/2-2/6/7 hexamer [29], may emerge as the mass rigidity overrides that of the soft template of the phospholipid bilayer (Figures 3H and 4).

Conclusions

This study has disclosed an unprecedented mode of interaction between a lipid bilayer and protein polymers. The data also provide biophysical evidence for the structural roles of septins in cortical morphogenesis, which have been previously suggested by genetic and cell biological studies.

The BAR domain proteins contained in the brain extract do not appear to play major roles in the transformation of giant PC-PI liposomes under our experimental conditions. The strict curvature sensitivity of the BAR domain, which favors smaller liposomes with steeper curvature ($\leq$0.1 μm in diameter), would not allow the proteins to bind to the gently curved membranes used in this study [10, 11, 32]. In contrast, septin filaments can take a wide range of curvature (0.3 μm–∞ in diameter) [6, 7] and interact with the giant liposomes (5–20 μm in diameter). Unlike other liposome-tubulating proteins, septins lack large membrane-binding domains, such as BAR, F-BAR/EFC, or PH (pleckstrin homology) [10–13, 28]. Although a single septin polypeptide or an oligomer may not have a high-affinity binding site for inositol phospholipids, a planar array of paired septin filaments assembled on a membrane template should exert a high binding avidity (Figure 4). The mass effect may also elicit the intrinsic curvature and rigidity that mold the lipid bilayer from the outside into a tubule with a certain range of positive curvature. In vivo, septins are commonly accumulated in reversed topology beneath specific plasma membrane ingressions or concavities, such as cleavage furrows that appear during cytokinesis, actin-rich arcs at the cell periphery, dendritic spine bases, and phagocytic cups [3–6, 21–24, 26]. Although the underpinning cytoskeletal organization remains to be analyzed [4], our data predict that these concavities are more or less stabilized by the presence of septin assemblies.

Protrusion of a tubule from a giant liposome requires a deformation force of several pN [19]. As has been proposed for the

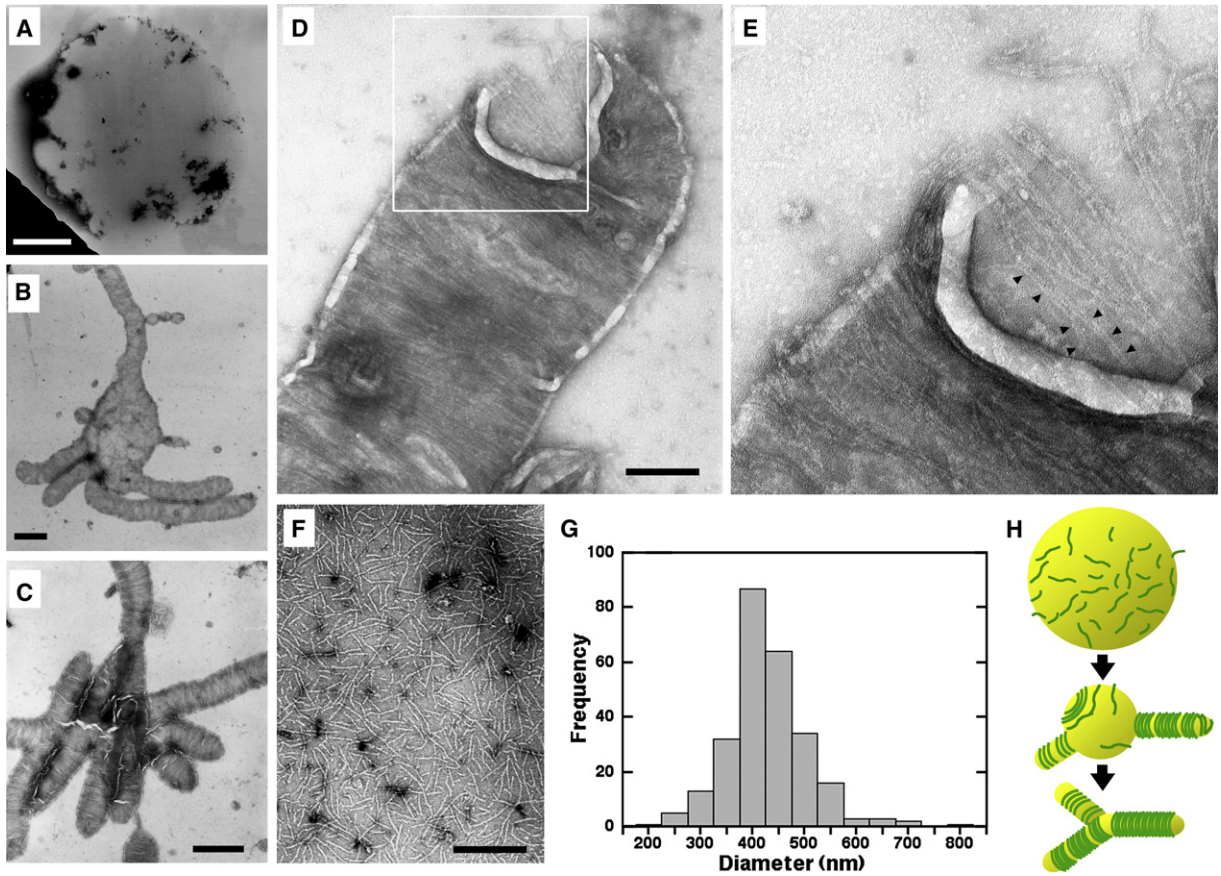

Figure 3. Uniform Bracing of the Lipid Bilayer by Circumferential Array of Septin Filaments

(A) Negative-stain EM image of a PC-PI liposome alone.

(B and C) Typical PC-PI liposomes (composition as in [A]) transformed by the active brain fraction (HA No. 11). As demonstrated by dark-field video microscopy, uniform tubules appeared to extend at the expense of the central spherical portion (B), and the transformation reaction was saturated when the entire surface was tubulated (C). Note that the filament array is sparse and less oriented at an early phase (B) and is dense and circumferentially oriented in a terminal phase (C).

(D and E) Higher magnifications of the tip of a tubule. An incidental rupture formed during preparation enabled the comparison of the septin filament array with or without an underlying membrane. The framed area in (D) is magnified in (E). Note that the septin filament array is composed of paired filaments (arrowheads) and wider bundles. A few free septin rods are also seen off the tubule.

(F) For comparison, [Sept2/6/7]n rods alone are shown in the same magnification as in (D).

Scale bars represent 1 μm in (A)–(C) and 200 nm in (D) and (F).

(G) Histogram of the diameter of the tubules estimated from the width of the ghosts collapsed on EM grids. The average diameter was 430 ± 79 nm (n = 261). (cf. Diameters of tubules induced with BAR or EFC domain proteins are approximately 20 and 60 nm, respectively [11, 12].)

(H) Schematic diagram of the liposome-septin interplay based on dark-field and EM observations. Septin rods (green) adhere to the surface of a giant liposome containing inositol phospholipids (yellow). The septin rods concentrated and oriented on the liposomal surface readily assemble into filaments, bundles, and arrays. The circumferential septin arrays reshape the spherical liposome into the intrinsic curvature they favor.

BAR and F-BAR/EFC domain proteins [10–12], the deformation energy may be derived from the attachment and assembly of the septin filament array on the liposomal surface. Whether mechanochemical force coupled to GTP/GDP exchange or GTP hydrolysis also contributes to the observed deformation, although not supported by our data, awaits future studies based on structural information at a higher resolution [7, 29]. Our experimental system and working model provide a starting point to design experiments to define the lipid-protein interfaces and to address the structural basis for higher-order septin assemblies.

Experimental Procedures

Giant liposomes were prepared as previously described [16, 19]. The brain extract was prepared as reported previously [33] with some modifications, and was further fractionated with a cation exchange column and a HA column. The recombinant septin complex and septin antibodies were prepared as previously described [6]. A liposome suspension and each sample solution such as the brain extract were gently mixed with each other in a glass flow cell [16]. Slowly moving liposomes were monitored at 25°C with a dark-field microscope (BHF, Olympus, Japan). For ultrastructural analysis, each sample was preobserved by dark-field microscopy and then was observed with a transmission electron microscope. See details in Supplemental Experimental Procedures.

Supplemental Data

Supplemental Data include Supplemental Experimental Procedures, seven figures, and two movies and can be found with this article online at http://www.current-biology.com/supplemental/S0960-9822(08)01685-0.

Acknowledgments

We are grateful to Yoshinori Yamakawa (Division for Medical Research Engineering, Graduate School of Medicine, Nagoya University) for mass

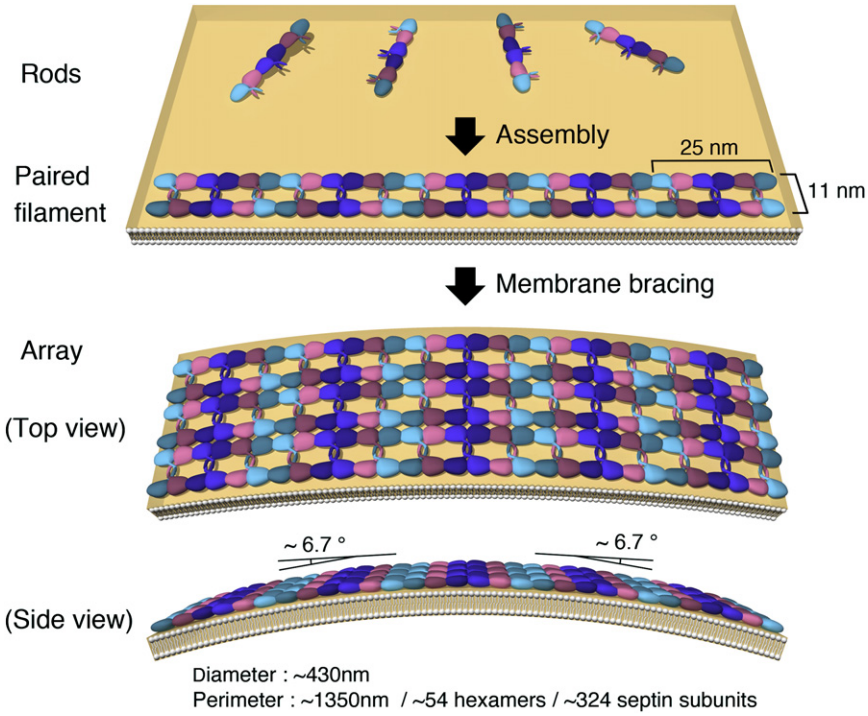

Figure 4. Working Model for the Septin Assembly on the Membrane Surface

Top: The hexameric septin rods and filaments are drawn according to the atomic structure and proposed models [2, 29, 34]. Sept2, 6, and 7 subunits are colored blue, pink, and cyan, respectively. Each septin rod weakly associates with the inositol phospholipid-containing lipid bilayer, but the short stretches of basic amino acids found only in Sept2 and Sept7 are dispensable for this step. The association not only concentrates but also spatially constrains and orients the septin rods, which facilitates the filament assembly. The carboxy-terminal coiled coil in each subunit points to the counterpart of the paired filament, as has been proposed for yeast septins [34]. The width of the paired filaments is 11 nm (cf. the interval of septin-based, electron-dense striations observed beneath the yeast bud neck membrane is ~10 nm [35]).

Middle and Bottom: As a septin filament array becomes larger, it adheres to the membrane more avidly. When the filament mass rigidity overrides that of the liposomal tension, the intrinsically favored curvature emerges. By simple arithmetic, an average-sized tubule (430 nm in diameter) is surrounded by 54 tandemly arrayed 25 nm long Sept7/6/2-2/6/7 hexamers, each bending 6.7° at the Sept2-Sept2 (NC) interface [29].

spectrometry, Toshiaki Gotoh (Technical Center of Nagoya University) for EM, Ai Tanigaki (Kyoto University) for the preparation of recombinant proteins, Hidetake Miyata (Tohoku University) for critical reading of the manuscript, Yoshiyuki Matsuura (Nagoya University) for valuable comments, and Hirokazu Hotani (JST) and Michio Homma (Nagoya University) for invaluable support and encouragement. This study was supported in part by a Grant-in-Aid (soft matter physics) from the MEXT of Japan and PRESTO from JST.

Received: June 18, 2008
Revised: December 1, 2008
Accepted: December 1, 2008
Published online: January 22, 2009

References

1. Janmey, P. (1995). Cell membranes and the cytoskeleton. In Structure and Dynamics of Membranes, Handbook of Biological Physics, R. Lipowsky and E. Sackmann, eds. (Amsterdam: Elsevier), pp. 805–849.
2. Weirich, C.S., Erzberger, J.P., and Barral, Y. (2008). The septin family of GTPases: architecture and dynamics. Nat. Rev. Mol. Cell Biol. *9*, 478–489.
3. Rodal, A.A., Kozubowski, L., Goode, B.L., Drubin, D.G., and Hartwig, J.H. (2005). Actin and septin ultrastructures at the budding yeast cell cortex. Mol. Biol. Cell *16*, 372–384.
4. Vrabioiu, A.M., and Mitchison, T.J. (2006). Structural insights into yeast septin organization from polarized fluorescence microscopy. Nature *443*, 466–469.
5. Barral, Y., and Mansuy, I.M. (2007). Septins: cellular and functional barriers of neuronal activity. Curr. Biol. *17*, R961–R963.
6. Kinoshita, M., Field, C.M., Coughlin, M.L., Straight, A.F., and Mitchison, T.J. (2002). Self- and actin-templated assembly of mammalian septins. Dev. Cell *3*, 791–802.
7. Farkasovsky, M., Herter, P., Voss, B., and Wittinghofer, A. (2005). Nucleotide binding and filament assembly of recombinant yeast septin complexes. Biol. Chem. *386*, 643–656.
8. Sackmann, E. (1995). Biological membranes architecture and function. In Structure and Dynamics of Membranes, Handbook of Biological Physics, R. Lipowsky and E. Sackmann, eds. (Amsterdam: Elsevier), pp. 1–65.
9. Rodriguez, O.C., Schaefer, A.W., Mandato, C.A., Forscher, P., Bement, W.M., and Waterman-Storer, C.M. (2003). Conserved microtubule-actin interactions in cell movement and morphogenesis. Nat. Cell Biol. *5*, 599–609.
10. Peter, B.J., Kent, H.M., Mills, I.G., Vallis, Y., Butler, P.J., Evans, P.R., and McMahon, H.T. (2004). BAR domains as sensors of membrane curvature: the amphiphysin BAR structure. Science *303*, 495–499.
11. Itoh, T., and De Camilli, P. (2006). BAR, F-BAR (EFC) and ENTH/ANTH domains in the regulation of membrane-cytosol interfaces and membrane curvature. Biochim. Biophys. Acta *1761*, 897–912.
12. Shimada, A., Niwa, H., Tsujita, K., Suetsugu, S., Nitta, K., Hanawa-Suetsugu, K., Akasaka, R., Nishino, Y., Toyama, M., Chen, L., et al. (2007). Curved EFC/F-BAR-domain dimers are joined end to end into a filament for membrane invagination in endocytosis. Cell *129*, 761–772.
13. Roux, A., Uyhazi, K., Frost, A., and De Camilli, P. (2006). GTP-dependent twisting of dynamin implicates constriction and tension in membrane fission. Nature *441*, 528–531.
14. Matsuo, H., Chevallier, J., Mayran, N., Le Blanc, I., Ferguson, C., Faure, J., Blanc, N.S., Matile, S., Dubochet, J., Sadoul, R., et al. (2004). Role of LBPA and Alix in multivesicular liposome formation and endosome organization. Science *303*, 531–534.
15. Hotani, H., Inaba, T., Nomura, F., Takeda, S., Takiguchi, K., Itoh, T.J., Umeda, T., and Ishijima, A. (2003). Mechanical analyses of morphological and topological transformation of liposomes. Biosystems *71*, 93–100.
16. Takiguchi, K., Nomura, F., Inaba, T., Takeda, S., Saitoh, A., and Hotani, H. (2002). Liposomes possess drastic capabilities for topological transformation. ChemPhysChem *3*, 571–574.
17. Vale, R.D., and Hotani, H. (1988). Formation of membrane networks in vitro by kinesin-driven microtubule movement. J. Cell Biol. *107*, 2233–2241.
18. Akashi, K.-I., Kinoshita, K., Jr., Miyata, H., and Itoh, H. (2000). Observation of a variety of giant vesicles under an optical microscope. In Giant Vesicles. Perspectives in Supramolecular Chemistry, *Vol. 6*, P.L. Luisi and P. Walde, eds. (New York: Wiley), pp. 45–48.
19. Inaba, T., Ishijima, A., Honda, M., Nomura, F., Takiguchi, K., and Hotani, H. (2005). Formation and maintenance of tubular membrane projections require mechanical force, but their elongation and shortening do not require additional force. J. Mol. Biol. *348*, 325–333.
20. Hsu, S.C., Hazuka, C.D., Roth, R., Foletti, D.L., Heuser, J., and Scheller, R.H. (1998). Subunit composition, protein interactions, and structures of the mammalian brain sec6/8 complex and septin filaments. Neuron *20*, 1111–1122.

21. Kinoshita, M. (2006). Diversity of septin scaffolds. Curr. Opin. Cell Biol. *18*, 54–60.
22. Xie, Y., Vessey, J.P., Konecna, A., Dahm, R., Macchi, P., and Kiebler, M.A. (2007). The dendritic spine-associated GTP-binding protein Septin 7 is critical for dendrite branching and dendritic spine morphology. Curr. Biol. *17*, 1746–1751.
23. Tada, T., Simonetta, A., Batterton, M., Kinoshita, M., Edbauer, D., and Sheng, M. (2007). Role of septin cytoskeleton in spine morphogenesis and dendrite development in neurons. Curr. Biol. *17*, 1752–1758.
24. Spiliotis, E.T., and Nelson, W.J. (2006). Here come the septins: novel polymers that coordinate intracellular functions and organization. J. Cell Sci. *119*, 4–10.
25. Ihara, M., Kinoshita, A., Yamada, S., Tanaka, H., Tanigaki, A., Kitano, A., Goto, M., Okubo, K., Nishiyama, H., Ogawa, O., et al. (2005). Cortical organization by the septin cytoskeleton is essential for structural and mechanical integrity of mammalian spermatozoa. Dev. Cell *8*, 343–352.
26. Huang, Y.W., Yan, M., Collins, R.F., DiCiccio, J.E., Grinstein, S., and Trimble, W.S. (2008). Mammalian septins are required for phagosome formation. Mol. Biol. Cell *19*, 1717–1726.
27. Tooley, A.J., Gilden, J., Jacobelli, J., Beemiller, P., Trimble, W.S., Kinoshita, M., and Krummel, M.F. (2009). Amoeboid T lymphocytes require the septin cytoskeleton for cortical integrity and persistent motility. Nat. Cell Biol. *11*, 17–26.
28. Blood, P.D., and Voth, G.A. (2006). Direct observation of Bin/amphiphysin/Rvs (BAR) domain-induced membrane curvature by means of molecular dynamics simulations. Proc. Natl. Acad. Sci. USA *103*, 15068–15072.
29. Sirajuddin, M., Farkasovsky, M., Hauer, F., Kuhlmann, D., Macara, I.G., Weyand, M., Stark, H., and Wittinghofer, A. (2007). Structural insight into filament formation by mammalian septins. Nature *449*, 311–315.
30. Zhang, J., Kong, C., Xie, H., McPherson, P.S., Grinstein, S., and Trimble, W.S. (1999). Phosphatidylinositol polyphosphate binding to the mammalian septin H5 is modulated by GTP. Curr. Biol. *9*, 1458–1467.
31. Casamayor, A., and Snyder, M. (2003). Molecular dissection of a yeast septin: distinct domains are required for septin interaction, localization, and function. Mol. Cell. Biol. *23*, 2762–2777.
32. McMahon, H.T., and Gallop, J.L. (2005). Membrane curvature and mechanisms of dynamic cell membrane remodelling. Nature *438*, 590–596.
33. Kinuta, M., Yamada, H., Abe, T., Watanabe, M., Li, S.A., Kamitani, A., Yasuda, T., Matsukawa, T., Kumon, H., and Takei, K. (2002). Phosphatidylinositol 4,5-bisphosphate stimulates vesicle formation from liposomes by brain cytosol. Proc. Natl. Acad. Sci. USA *99*, 2842–2847.
34. Bertin, A., McMurray, M.A., Grob, P., Park, S.-S., Garcia, G., III, Patanwala, I., Ng, H., Alber, T., Thorner, J., and Nogales, E. (2008). Saccharomyces cerevisiae septins: supramolecular organization of heterooligomers and the mechanism of filament assembly. Proc. Natl. Acad. Sci. USA *105*, 8274–8279.
35. Byers, B., and Goetsch, L. (1976). A highly ordered ring of membrane-associated filaments in budding yeast. J. Cell Biol. *69*, 717–721.